HHS Public Access

Author manuscript

Cell. Author manuscript; available in PMC 2017 January 28.

Published in final edited form as:

Cell. 2016 January 28; 164(3): 526–537. doi:10.1016/j.cell.2015.12.037.

Cell-Type-Specific Control of Brainstem Locomotor Circuits by Basal Ganglia

Thomas K. Roseberry[1,2,#], **A. Moses Lee**[1,2,3,#], **Arnaud L. Lalive**[1], **Linda Wilbrecht**[4], **Antonello Bonci**[5,6,7], and **Anatol C. Kreitzer**[1,2,3,8,*]

[1]The Gladstone Institutes, San Francisco, CA 94158 USA

[2]Neuroscience Graduate Program, University of California, San Francisco, CA 94158 USA

[3]Medical Scientist Training Program, University of California, San Francisco, CA 94158 USA

[4]Department of Psychology, University of California, Berkeley, CA 94720 USA

[5]Intramural Research Program, Synaptic Plasticity Section, National Institute for Drug Abuse, Baltimore, MD 21224 USA

[6]Solomon H. Snyder Department of Neuroscience, Johns Hopkins University, Baltimore, MD 21205 USA

[7]Department of Psychiatry, Johns Hopkins University, Baltimore, MD 21287 USA

[8]Departments of Physiology and Neurology, University of California, San Francisco, CA 94158 USA

Summary

The basal ganglia (BG) are critical for adaptive motor control, but the circuit principles underlying their pathway-specific modulation of target regions are not well understood. Here, we dissect the mechanisms underlying BG direct- and indirect-pathway-mediated control of the mesencephalic locomotor region (MLR), a brainstem target of the BG that is critical for locomotion. We optogenetically dissect the locomotor function of the three neurochemically-distinct cell types within the MLR: glutamatergic, GABAergic, and cholinergic neurons. We find that the glutamatergic subpopulation encodes locomotor state and speed, is necessary and sufficient for locomotion, and is selectively innervated by BG. We further show activation and suppression, respectively, of MLR glutamatergic neurons by direct and indirect pathways, which is required for bidirectional control of locomotion by BG circuits. These findings provide a fundamental

*correspondence to: akreitzer@gladstone.ucsf.edu.
#contributed equally

Author contributions: A.M.L conceptualized and initiated the project in the laboratory of A.B., continued the project in the laboratory of L.W., and brought the project to the laboratory of A.C.K., where he conducted experiments together with T.K.R. and co-wrote the manuscript. T.K.R. performed experiments, analyzed all data, and co-wrote the manuscript. A.L.L. performed slice electrophysiology recordings. A.C.K. designed experiments, supervised the project, and co-wrote the manuscript.

understanding of how the BG can initiate or suppress a motor program through cell-type-specific regulation of neurons linked to specific actions.

Introduction

The ability to move through the environment to obtain energy, escape predators, and reproduce is fundamental for an animal's survival. In vertebrates, phylogenetically-conserved brainstem and spinal circuitry mediates the control of axial muscles and limbs that drive locomotion (Garcia-Rill, 1986; Grillner et al., 2005; Orlovsky, 1999; Shik et al., 1966a). In addition, upstream circuitry responsible for deciding when and how to move must be engaged. The BG has long been hypothesized to be a key arbitrator of the decision process that results in goal-directed locomotion (Garcia-Rill, 1986; Grillner et al., 2008; Hikosaka et al., 2000). Canonically, the BG consists of two pathways which separate at the level of the striatum, the main input nucleus of the BG. Striatal medium spiny neurons (MSNs) expressing the dopamine D1 receptor mark the direct pathway (dMSNs) and are proposed to facilitate movement, and MSNs expressing the dopamine D2 and adenosine 2a (A2a) receptor mark the indirect pathway (iMSNs) and are proposed to suppress movement (Albin et al., 1989; DeLong, 1990; Kreitzer and Malenka, 2008). These pathways re-converge in the substantia nigra pars reticulata (SNr), the primary output nucleus of the basal ganglia in rodents, which provides tonic inhibition of downstream structures responsible for the execution of motor programs (Hikosaka et al., 2000). Recent work from our laboratory has established that optogenetic activation of dMSNs increases locomotion, whereas activation of iMSNs suppresses locomotion (Kravitz et al., 2010). However, the effect of basal ganglia circuitry on downstream targets controlling locomotion remains unknown.

The BG locomotor command is thought to be relayed to spinal cord central pattern generators through the MLR, a brainstem area first described in 1966 by Shik and colleagues (Shik et al., 1966b). The MLR is defined functionally as a mesencephalic region in which increasing intensities of electrical stimulation induce a transition from a stationary state to walking and then running with short latencies (Shik et al., 1966a; Shik et al., 1966b). In mammals, the MLR overlaps with the cuneiform nucleus (Cun), mesencephalic reticular nucleus (MRN) and pedunculopontine tegmental nucleus (PPTg) (Garcia-Rill et al., 1986; Ryczko and Dubuc, 2013). The MLR is comprised of three neurochemically distinct cell types: glutamatergic, GABAergic, and cholinergic (Martinez-Gonzalez et al., 2011). Although the major cell populations of the MLR give rise to ascending projections into the forebrain that may be relevant for reward, arousal, and cortical state (Ehrich et al., 2014; Grace, 2010; Lee et al., 2014; Thompson and Felsen, 2013), the control of locomotion appears to be driven through descending outputs, as locomotion is intact in decerebrate animals (Bedford et al., 1992; Whelan, 1996).

Previous work has demonstrated that subsets of neurons in the MLR are correlated with locomotion (Lee et al., 2014; Norton et al., 2011; Thankachan et al., 2012). However, less is known about the activity of identified MLR glutamate neurons in vivo, and whether their activity is actually necessary for locomotion. Moreover, the function of the cholinergic and

GABAergic populations during locomotion is not clear. To investigate the locomotor function of MLR cell types and their control by BG circuitry, we combined cell-type-specific optogenetic manipulations, *in vivo* single-unit recording from identified cells, viral-based circuit mapping, and high-resolution behavioral assays to explore how signals from the BG are transduced into locomotion through the MLR. Our results highlight the functional differences among cell types in the MLR, and the remarkable specificity of BG-brainstem projections. In addition to defining the pathway through which the BG regulate locomotion, these results provide a more general framework for how the BG can initiate or suppress action by specific modulation of neuronal sub-types associated with a motor program.

Results

Identification of Mouse MLR

To identify the location of the MLR in mouse, we used a head-fixed preparation that allowed the subject to walk on a spherical treadmill (trackball) suspended by air (Figure 1A). All subsequent experiments are performed using this preparation unless otherwise stated. Five seconds of electrical stimulation at 20 Hz using a bipolar electrode placed near the PPTg elicited a transition from a stationary state to running (Figures 1B and 1C; mean latency to movement onset: 1580 ± 165 ms) thus confirming the existence of the MLR. To determine the anatomical extent of the MLR, we systematically stimulated across multiple areas in the mesencephalon and histologically confirmed electrode placements that elicited locomotion with latencies of <2 sec. These experiments confirmed that the MLR overlaps with the Cun, PPTg, and MRN (Figure 1D), consistent with other species (Ryczko and Dubuc, 2013).

Bidirectional Modulation of MLR Neurons by the BG

The direct and indirect pathways of the BG exert opposing effects on locomotion (Bateup et al., 2010; Kravitz et al., 2010). To determine how these pathways modulate activity in the MLR, we injected D1-Cre mice, to activate dMSNs, or A2a-Cre mice, to activate iMSNs, with adeno-associated virus for Cre-dependent expression of channelrhodopsin (DIO-ChR2) into striatum. We then recorded from well-isolated, single units in the MLR while stimulating ChR2-expressing neurons in the striatum (Figures 1E and 1I). Unilateral dMSN stimulation resulted in contraversive locomotion when initiated while the mouse was stationary (mean latency to movement onset: 565 ± 78 ms; Figure 1F). Although a majority of MLR neurons increased their firing rate in response to dMSN stimulation, a large fraction was either unmodulated or inhibited (Figures 1F and 1G). We continued to record these neurons after the stimulation session as the mice spontaneously ran on the trackball. Receiver Operating Characteristic (ROC) analysis revealed that neurons excited by dMSN stimulation were also significantly more predictive of the running state than the stationary state when compared to the dMSN-unmodulated or dMSN-inhibited neurons (Figure 1G; $p < 0.01$, Kruskal-Wallis one-way ANOVA, $\chi^2_{2,39} = 15.96$, with Dunn-Sidak post test). Conversely, 5 seconds of bilateral iMSN stimulation resulted in a transition from running to the stationary state (mean deceleration onset: 651 ± 34 ms) and inhibition of a majority of recorded units in MLR (Figures 1I and 1J). ROC analysis of spontaneous running revealed

no relationship between iMSN modulation and prediction of locomotor state (Figure 1J). These results demonstrate that the BG can modulate activity within the MLR, although the responses within MLR are heterogeneous.

Functional Dissection of MLR Cell Types

To better understand the relationship between MLR cell types and locomotion, we next examined how optogenetic activation of each cell type affects locomotion. Glutamatergic or GABAergic neurons were transduced by injecting Cre-inducible virus expressing ChR2-YFP into vGLUT2-Cre or vGAT-Cre mice (Figures 2B and 2C). Whole-cell recordings confirmed that infected neurons released either glutamate or GABA by blocking EPSCs or IPSCs, respectively, with antagonists (Figure S1A –D). Cholinergic neurons were labeled in transgenic mice expressing ChR2-YFP under the choline acetyltransferase promoter (Zhao et al., 2011) (Figure 2A). 10 ms light pulses delivered at 20 Hz to the glutamatergic population for 5 seconds elicited robust locomotion (Figures 2F and 2I) at significantly shorter latencies than electrical stimulation (mean movement onset 211 ± 22 ms, $p < 0.01$, Wilcoxon rank sum). The speed reached at the end of stimulation was graded by stimulation frequency (Borgius et al., 2010; Lee et al., 2014), a canonical feature of the MLR (Figure 2K). In contrast, stimulation of the GABAergic population during running caused deceleration (mean deceleration onset: 837 ± 99 ms, Figure 2H and S2F), but no change if the mouse was stationary at the beginning of stimulation (Figure 2E and 2J). ChAT stimulation resulted in a significant increase in speed during trials when the mouse was running, but not when the mouse was stopped (Figures 2D, 2G, 2J and S2F). Thus, ChAT neurons appear to modulate locomotion, but are not sufficient to drive locomotion at short latencies. This modulation did not appear to result from co-release of glutamate or GABA, as no EPSCs or IPSCs were observed in the MLR during light stimulation in slice (Figure S1E). eYFP controls showed no significant changes in locomotion (Figure 2J and S2F). Together, these results indicate that increased activity within the glutamatergic population alone is sufficient to drive locomotion.

MLR Glutamatergic Neurons Encode Locomotion

To understand how MLR glutamatergic neuron firing relates to locomotion, we injected vGLUT2-Cre mice with DIO-ChR2 in the MLR to optogenetically identify glutamatergic neurons and record their activity during spontaneous locomotion (Figure 3A). Experiments began with an identification session in which 473 nm light was pulsed for 10 ms at 1–2 Hz while evoked single-unit activity was recorded. Well-isolated single-units that displayed increased firing within 5 ms of light onset and had spontaneous and light-evoked waveform correlations > 0.9 (Pearson's correlation coefficient) were considered glutamatergic (Figure 3B–D). A locomotor session followed, in which the same single-unit activity was recorded during spontaneous running (Figure 3E). A second identification session was run after the locomotor session to ensure that there was no drift. Neurons that were held for all three sessions (based on cluster analysis, see Methods) and found to be inside the functional boundaries of the MLR were kept for analysis (Figure 3B–D). To quantify how closely these neurons encode the running state, we performed ROC analysis on the firing rate and speed data. The firing rate of individual MLR glutamatergic neurons was highly predictive of the running state (Figure 3F). In contrast, unidentified neurons from a separate cohort of mice

displayed significantly lower AUCs, indicating functional heterogeneity among MLR neuronal subpopulations (Figure 3F). To further dissect this result, we tested the locomotor-predictive MLR glutamatergic neurons for correlations with speed using a linear regression model. This analysis yielded two distinct populations: one that predicts locomotor state alone and one that predicts state and correlates with speed (Figure 3G). We next tested whether glutamatergic neuron firing rate was predictive of locomotor starts. Glutamatergic neurons as a population increased their firing rate prior to the onset of a spontaneous locomotor start (Figure 3H). However on individual trials, spiking increase onset was highly variable and an absolute threshold at which spiking would correlate with running onset was not observed (Figure 3H inset). Therefore we tested the prediction that spiking increases during the stationary state would result in an increased probability of running onset. Indeed, increased firing rate during the stationary state was correlated with an increase in the probability of a start occurring within the next second (Figure 3I, Pearson's, $p < 0.01$). This suggests that at the individual level, glutamatergic neurons do not predict the timing of locomotion onset. Rather, these neurons contribute to an increased probability of locomotion that is read out from the population. These findings indicate that MLR glutamatergic activity is tightly linked with and predictive of an animal's locomotor state and speed.

MLR Glutamatergic Neurons are Required for Spontaneous Locomotion

Because activity in MLR glutamatergic neurons is sufficient for locomotion and encodes locomotor state and speed, we next tested if they are necessary for spontaneous running. Previous experiments examining inhibition of the MLR have reported mixed effects on locomotion, most likely due to the long term and non-specific effects of pharmacological interventions (Saper et al., 1979; Sinnamon et al., 1987). To specifically inhibit the glutamatergic population on millisecond timescale, we expressed halorhodopsin (eNpHR3.0) under the CaMKIIα promoter, which targets glutamatergic neurons in the MLR with high selectivity (Lee et al., 2014) (Figure 4A and S3A–B). Photo-inhibition of MLR glutamatergic neurons caused running animals to rapidly decelerate, often to a full stop (mean deceleration onset 835 ± 103 ms; Figure 4B–D), whereas control animals showed only a gradual decrease in mean speed over time, consistent with a low baseline probability of spontaneous stopping. This result indicates that MLR glutamatergic neurons are necessary for spontaneous locomotion.

MLR GABAergic Neurons Suppress Activity in the MLR

Because activation of the MLR GABAergic population decreased locomotion, we next examined whether these neurons locally inhibited other MLR neurons. In MLR slices prepared from mice expressing ChR2-eYFP in GABAergic neurons, IPSCs and inhibition of spiking were observed during whole-cell recordings from ChR2-eYFP-negative cells in response to optogenetic stimulation (Figures S1C–DD and S4A). *In vivo* recordings during optogenetic stimulation of MLR GABA neurons demonstrated that the majority of non-light-sensitive neurons were inhibited for the duration of illumination (Figures S4B–CC). Because activity in MLR glutamatergic neurons is required for running (Figure 4), deceleration and stopping due to optogenetic activation of GABAergic neurons is likely due, in part, to local inhibition of MLR glutamatergic neurons. However, in vivo recordings from optogenetically-identified MLR GABA neurons during spontaneous locomotion revealed

heterogeneous responses, indicating additional complexity in the composition and function of this subpopulation (Figure S4D).

Brain-Wide Tracing of Monosynaptic Inputs to MLR Glutamatergic and GABAergic Neurons

We next tested the connection strength between the BG and the two MLR populations displaying the most robust effects on locomotion. In theory, BG-driven locomotion could be initiated by disinhibition of MLR glutamatergic neurons (Grillner et al., 2008; Hikosaka et al., 2000) or inhibition of GABAergic neurons. A difference in connection strength from the BG could discriminate between these possibilities. We used a cell-type-specific G-deleted rabies viral strategy to map neurons that directly target MLR glutamatergic or GABAergic neurons (Wall et al., 2013). vGLUT2-Cre or vGAT-Cre mice were injected with an AAV encoding rabies virus glycoprotein (RG) and a separate virus encoding a Cre-inducible avian receptor (TVA-mCherry) in the MLR on Day 1. Only Cre-expressing cells will express the TVA receptor which is required for rabies transduction. On Day 14, mice were injected in the same area with modified rabies virus. 9 days later mice were perfused and brains processed (Figure 5A). Retrograde trans-synaptic labeling from MLR glutamatergic neurons revealed dense projections from several BG nuclei, whereas few if any projections targeted MLR GABAergic neurons (Figure 5C–F). A brain-wide survey of long-range projections to these cell types revealed another strong projection to MLR glutamatergic neurons from the central amygdala and oval bed nucleus of the stria terminalis (ovBNST), GABAergic nuclei that could play a role in fear and anxiety-associated behaviors such as freezing (Figure 5F) (LeDoux, 2000). Major MLR GABAergic-targeting regions included the superior colliculus, dorsal raphe, laterodorsal tegmentum and ovBNST. Together, these results suggest a specific role for MLR glutamatergic neurons in the control of locomotion by upstream targets and notably the BG.

Modulation of MLR Glutamatergic Neurons is Required for Bidirectional Control of Locomotion by BG Circuitry

In order to test how the direct and indirect pathways specifically modulate the MLR glutamatergic population, we optogenetically identified MLR glutamatergic neurons and recorded their activity while simultaneously stimulating dMSNs or iMSNs in striatum. We expressed ChR2 in dMSNs or iMSNs using Cre-dependent viruses injected into striatum of D1- or A2A-Cre mice. In the same mice, we expressed ChR2 in MLR glutamatergic neurons for optogenetic identification using virus expressing ChR2 under the CaMKIIα promoter (Figure 6A and 6E). Each experiment began with an identification session to find putative glutamatergic neurons based on the criteria listed previously. CaMKIIα-ChR2 had similar light responses to the vGLUT2-Cre::DIO-ChR2 strategy (Figure S3C–D). After MLR neuron identification, we stimulated striatal dMSNs or iMSNs (5 second continuous light) while recording MLR glutamatergic neuron activity. This was followed by a second MLR neuron identification session. Fiber and electrode placements were confirmed post hoc (Figure S5A–D).

Unilateral dMSN stimulation significantly increased firing rate in 25/26 identified MLR glutamatergic neurons (Figure 6B). In each case, the increase in firing rate preceded

movement onset (mean latency to excitation: 176 ± 18 ms; Figures 6B, S5J–K). In contrast, bilateral iMSN stimulation delivered while the mouse was running significantly decreased the firing rate in 25/27 identified MLR glutamatergic neurons (Figure 6F). Deceleration was preceded by decreases in firing rate in the majority of identified MLR glutamatergic neurons (mean latency to inhibition, 460 ± 48 ms; Figures 6F, S5H–I). To better compare dMSN and iMSN stimulation latencies (Freeze et al., 2013; Oldenburg and Sabatini, 2015) we analyzed trials in which the mouse was stationary prior to iMSN stimulation. Latencies to inhibition were markedly shorter relative to running trials (latency to inhibition, 276 ± 30 ms, Figure S5G), yet still longer than excitation during dMSN stimulation. Finally, in contrast to data obtained from identified glutamatergic neurons, unidentified MLR neurons displayed significantly more heterogeneous responses to stimulation of either pathway (Figures 6B and 6F), indicating that more complex circuit dynamics are controlling the activity of other neuronal subpopulations in MLR.

Given that MLR glutamatergic neurons are sufficient for locomotion, correlated with locomotion, and modulated by the BG, we next asked whether they are necessary for BG-driven locomotion. To investigate this, we expressed eNpHR3.0 in the MLR under the CaMKIIα promoter, and ChR2 in dMSNs using Cre-dependent virus injected into striatum of D1-Cre mice (Figures 6D and S5E–F). Unilateral activation of dMSNs for 10 seconds elicited locomotion throughout the duration of the stimulation (Figure 6D). During interleaved trials, MLR glutamatergic neurons were optogenetically inhibited from 5–10 sec after the onset of dMSN stimulation, which led to a striking decrease in running speed, despite continued activation of dMSNs (Figure 6D). As a control, we looked at 1000 time points when the mouse had been stationary for the same amount of time as ‘dMSN stim only’ and ‘dMSN stim + MLR inhibition’ trials and found that this similar baseline resulted in a spontaneous speed trajectory that did not resemble either stimulation condition. No change in locomotion was observed in trials without MLR inhibition, or when light was delivered to MLR glutamatergic neurons expressing only YFP. Qualitatively similar results were observed in freely-moving mice (Figure S6).

We then tested whether inhibition of MLR neurons was necessary for locomotor suppression observed with iMSN stimulation. In these experiments, we expressed ChR2 in the MLR under the CaMKIIα promoter, and ChR2 in dMSNs using Cre-dependent virus injected into striatum of A2a-Cre mice (Figure 6G and S5A–B). Bilateral activation of iMSNs for 10 seconds induced locomotor suppression throughout the duration of the stimulation (Figure 6H). This arrest was completely reversed by 20 Hz optical stimulation of MLR glutamatergic neurons delivered 5 seconds after the onset of the 10 second iMSN stimulation (Figure 6H). This reversal was not observed in eYFP controls. In addition, control trials with similar baselines but no stimulation of the iMSN or MLR glutamatergic neurons showed no changes in running speed. Taken together, these results demonstrate that bidirectional control of locomotion by basal ganglia circuitry requires modulation of MLR glutamatergic neurons.

Discussion

Cell-Type-Specific Control of Locomotion by MLR Neurons

Previous work has shown that the MLR has robust descending projections to the gigantocellular nucleus (Martinez-Gonzalez et al., 2014; Mitani et al., 1988; Rye et al., 1988), also referred to as the ventromedial medulla (Sherman et al., 2015; Skinner et al., 1990). In addition, MLR axons and terminals have been found in the pontine reticular formation (Takakusaki et al., 1996) and nucleus pontine oralis (Garcia-Rill et al., 2001). Collectively, these nuclei form the origin of reticulospinal tracts that project into the spinal cord and mediate various aspects of posture and movement. There may also be spinally-projecting glutamatergic neurons within the boundaries of the MLR (Sherman et al., 2015). Indeed, lesion of the major non-spinal targets of the MLR do not reduce gross aspects of locomotor function (Noga et al., 1988; Sherman et al., 2015), raising the possibility that the MLR acts as a comprehensive coordinator of locomotion.

Our optogenetic dissection of MLR cell types revealed that only the glutamatergic population was sufficient to elicit running at short latencies, consistent with the classical definition of the MLR (Grillner et al., 2008; Ryczko and Dubuc, 2013; Shik et al., 1966b). This is in agreement with a recent study showing that cells targeted with CaMKIIα-ChR2 virus in the MLR could elicit running (Lee et al., 2014), and consistent with current hypotheses about brainstem locomotor control (Grillner et al., 2005; Sherman et al., 2015). In spite of previous experiments that were unable to stop locomotion via pharmacologic inhibition or lesion of the MLR (Saper et al., 1979; Sinnamon et al., 1987), rapid optogenetic suppression of the MLR glutamatergic population revealed that these neurons are indeed necessary for locomotion.

In contrast to glutamatergic neurons, the MLR GABAergic population caused cessation of locomotion. While this population encoded both running and stationary states (Figure S4), the deceleration and stopping observed during stimulation could be due, in part, to local inhibition of the MLR glutamatergic population. However inhibition of downstream targets is also a possibility. MLR GABA neurons received dense input from limbic centers (Amygdala, PAG and BNST), suggesting that they could be involved in fear-related behavior. GABAergic neurons in neighboring regions have also been shown to suppress locomotion (Giber et al., 2015; Shang et al., 2015), suggesting that the function of GABAergic cells at this level of the mesencephalon share similar functions.

Finally, stimulation of the MLR cholinergic population demonstrated that while these neurons can modulate locomotion, they are insufficient to initiate it with short latency. This population has previously been hypothesized to control locomotion (Skinner et al., 1990). PPTg cholinergic neurons send projections to the ventromedial medulla, depolarizing glutamatergic cells that in turn project to reticulospinal neurons (Brudzynski et al., 1988; Mamiya et al., 2005; Smetana et al., 2010). However other work has shown that these neurons play a major role in gating brain state as part of the ascending reticular activating system (Mena-Segovia et al., 2008; Van Dort et al., 2015). Because locomotion and brain state are clearly linked (Lee et al., 2014; Niell and Stryker, 2010), the timecourse of behavioral changes is critical to consider.

Non-canonical Projections from the BG and Other Nuclei

The BG interface strongly with the MLR, making reciprocal connections from most of its nuclei (Martinez-Gonzalez et al., 2011; Mena-Segovia et al., 2004). Our rabies tracing showed that it is the glutamatergic population — and not the GABAergic population — that is the primary target of these BG connections. In addition, our tracing highlighted a number of non-canonical pathways to the MLR from the BG (EP, GPe, STN) to MLR glutamatergic neurons. The STN projection is of interest, as it is predicted to arrive in the MLR prior to the classical indirect pathway signal through the SNr, and it should drive activity in the opposite direction. Indeed, a small minority of cells displayed a small uptick in firing rate prior to inhibition (Figure 6F), consistent with the idea that this pathway modulates MLR activity, perhaps as a brief arousal signal prior to suppression of locomotion.

Striatal neurons also send projections directly to MLR glutamate neurons. Interestingly, the PPTg, one of the MLR nuclei, also sends projections back to the striatum (Wall et al., 2013) thus forming a reciprocal connection. As iMSNs do not project past the GPe, it is most likely the dMSN population that sends axons to the MLR. As this connection is GABAergic, these cells may form synapses onto the small number of glutamatergic neurons that fire most during the stationary state. dMSNs in the DMS could therefore coordinate the initiation of locomotion by directly inhibiting these cells

Comparison to Other BG Targets

The BG output nuclei also project to the thalamus and superior colliculus (SC) (Bosch-Bouju et al., 2013; Hikosaka et al., 2000), enabling broad control of cortical and brainstem circuitry. Recent work has shown that direct and indirect pathway stimulation increases and decreases firing rates in motor cortex, respectively, along with increasing and decreasing lever press frequency in an operant task (Oldenburg and Sabatini, 2015). However, the principles underlying BG control of thalamus and cortex remain largely mysterious (Bosch-Bouju et al., 2013; Goldberg et al., 2013). In contrast, the BG has long been proposed to act as a ‘gate’ for motor behaviors originating from the SC, such as turning and saccades (Girard and Berthoz, 2005; Hikosaka et al., 2000), as the SNr is known to exert tonic inhibitory control over the SC (Chevalier et al., 1984). To initiate an orienting movement, SNr inhibition to the contralateral SC is released allowing input from the cortex to excite SC neurons, which in turn drive the action (Hikosaka and Wurtz, 1983). The SC is topographically organized by the visual field (Schiller and Stryker, 1972), as are SNr inputs (Hikosaka and Wurtz, 1983). Because of this association, the BG has been hypothesized to play a role in deciding important targets for orienting (Hikosaka et al., 2006). Between this SC-mediated orienting and MLR-mediated running, these brainstem BG targets are fully capable of defining locomotor trajectories, consistent with decortication studies (Bjursten et al., 1976). In addition, our rabies result demonstrates that the SC connects directly with the MLR, consistent with previous studies (Martinez-Gonzalez et al., 2011; Perkins et al., 2014; Redgrave et al., 1987), providing another connection through which BG-brainstem connections could exert navigational control.

BG Pathway-Specific Selection and Suppression of Action

Our cell-type-specific recordings from MLR during iMSN and dMSN stimulation reveal a remarkable degree of homogeneity in the glutamatergic population response. The majority of responses preceded changes in locomotion, suggesting that they were causally related to behavior. In support of this, inhibition of the glutamatergic population during dMSN-induced locomotion caused the mouse to stop running. Although the functional responses observed in SNr in response to striatal stimulation are complex (Freeze et al., 2013), the signal becomes surprisingly uniform at the level of the MLR glutamatergic population. Together with the rabies results, this indicates a highly specific connection between BG and locomotor-encoding MLR neurons.

Given its ability to drive a robust behavioral output, the MLR represents an ideal system for understanding the BG's role in action selection. Classical models of the BG suggest that movement occurs when the direct pathway is active and cessation of movement occurs with indirect pathway activation. However, both pathways appear to be co-active during normal movement (Cui et al., 2013). One possibility is that different information is encoded in the direct and indirect pathway circuits, which together form the basis for action selection. For example, indirect pathway activity could encode information about competing behavioral choices. Our data suggests that the balance of activity between the direct and indirect pathways is represented in the firing rate of glutamatergic MLR neurons, which is predictive of the initiation of running and sufficient to drive graded locomotion. Further experiments can help clarify the validity of this model for the MLR and other BG output structures.

Experimental Procedures

Subjects—86 adult transgenic or wild-type mice on a C57BL/6 background aged 50 to 100 days were used in the experiments. vGLUT2-Cre (Jackson Stock# 016963), vGAT-Cre (Jackson Stock# 016962), ChAT-ChR2 (Jackson Stock# 014546) and wild-type C57BL/6 (Jackson Stock# 000664) mice were used for optogenetic stimulation, inhibition or recording experiments. vGLUT2-Cre and vGAT-Cre were used for rabies tracing experiments. D1-Cre mice (GENSAT #030778-UCD) were used for dMSN stimulation while recording responses from identified glutamatergic neurons or inhibiting the MLR. A2a-Cre mice (GENSAT #031168-UCD) were used for iMSN stimulation while recording identified responses from identified glutamatergic neurons or stimulating the MLR. vGLUT2-Cre mice crossed into an Ai14 line (Jackson Stock #007914) were used for confirmation of CAMKIIα expression in vGLUT2-expressing neurons.

Surgery—For dMSN or iMSN activation, AAV5-EF1α-DIO-ChR2-eYFP (UPenn) was injected into the dorsomedialstriatum at (0.8 mm AP/− 2.5 DV/± 1.5 ML) measured from Bregma. For activation of cells in the MLR AAV5-EF1α-DIO-ChR2-eYFP or AAV5-CAMKIIα-ChR2-eYFP (for glutamatergic neurons) was injected at (−0.8 mm AP/−3.6 DV/± 1.2 ML), measured from Lambda. Where appropriate, fiber optic ferrules were implanted 0.5 mm above the injection sites. Virus was allowed to express for 2–6 weeks after which mice were implanted with a custom built stainless steel headbar for head fixation. 7 to 10 days later mice were habituated to the trackball until able to run normally at which point recordings would take place.

Recording and Optogenetics—Extracellular recordings were performed using a Plexon data acquisition system (Plexon Inc.). A blue laser (473 nm; 100 mW; OEM) was triggered through a TTL pulse generator (PulseBlaster, SpinCore Technologies, Inc). Trackball movement was read by optical mice fed into custom MATLAB (Mathworks) data acquisition software.

Data Analysis—Data analyses were carried out using built-in (NeuroExplorer, Plexon Inc.) and custom-built software in Matlab (MathWorks). Single units were sorted into clusters using commercially available software (Plexon Offline Sorter 2.4, Plexon Inc.). See Supplemental methods for further details.

Supplementary Material

Refer to Web version on PubMed Central for supplementary material.

Acknowledgments

We thank Delanie Schulte for assistance with genotyping, histology, and microscopy, and the Kreitzer Lab for comments on the manuscript. This work was funded by NIH R01 NS064984 and P01 DA010154 to A.C.K., F31 NS092253 to T.K.R., 5T32GM007618-38 to A.M.L., RR018928 to the Gladstone Institutes, a grant from the Swiss National Science Foundation to A.L.L., funds from the State of California to L.W., and NIDA Intramural program for A.B.

References

Albin RL, Young AB, Penney JB. The Functional-Anatomy of Basal Ganglia Disorders. Trends in Neurosciences. 1989; 12:366–375. [PubMed: 2479133]

Bateup HS, Santini E, Shen W, Birnbaum S, Valjent E, Surmeier DJ, Fisone G, Nestler EJ, Greengard P. Distinct subclasses of medium spiny neurons differentially regulate striatal motor behaviors. Proceedings of the National Academy of Sciences of the United States of America. 2010; 107:14845–14850. [PubMed: 20682746]

Bedford TG, Loi PK, Crandall CC. A model of dynamic exercise: the decerebrate rat locomotor preparation. Journal of applied physiology. 1992; 72:121–127. [PubMed: 1537705]

Bjursten LM, Norrsell K, Norrsell U. Behavioural repertory of cats without cerebral cortex from infancy. Experimental brain research. 1976; 25:115–130. [PubMed: 1278272]

Borgius L, Restrepo CE, Leao RN, Saleh N, Kiehn O. A transgenic mouse line for molecular genetic analysis of excitatory glutamatergic neurons. Molecular and cellular neurosciences. 2010; 45:245–257. [PubMed: 20600924]

Bosch-Bouju C, Hyland BI, Parr-Brownlie LC. Motor thalamus integration of cortical, cerebellar and basal ganglia information: implications for normal and parkinsonian conditions. Front Comput Neurosci. 2013; 7:163. [PubMed: 24273509]

Brudzynski SM, Wu M, Mogenson GJ. Modulation of locomotor activity induced by injections of carbachol into the tegmental pedunculopontine nucleus and adjacent areas in the rat. Brain research. 1988; 451:119–125. [PubMed: 3251577]

Chevalier G, Vacher S, Deniau JM. Inhibitory nigral influence on tectospinal neurons, a possible implication of basal ganglia in orienting behavior. Experimental brain research. 1984; 53:320–326. [PubMed: 6705865]

Cui G, Jun SB, Jin X, Pham MD, Vogel SS, Lovinger DM, Costa RM. Concurrent activation of striatal direct and indirect pathways during action initiation. Nature. 2013; 494:238–242. [PubMed: 23354054]

DeLong MR. Primate models of movement disorders of basal ganglia origin. Trends in neurosciences. 1990; 13:281–285. [PubMed: 1695404]

Ehrich JM, Phillips PE, Chavkin C. Kappa opioid receptor activation potentiates the cocaine-induced increase in evoked dopamine release recorded in vivo in the mouse nucleus accumbens. Neuropsychopharmacology : official publication of the American College of Neuropsychopharmacology. 2014; 39:3036–3048. [PubMed: 24971603]

Freeze BS, Kravitz AV, Hammack N, Berke JD, Kreitzer AC. Control of basal ganglia output by direct and indirect pathway projection neurons. J Neurosci. 2013; 33:18531–18539. [PubMed: 24259575]

Garcia-Rill E. The basal ganglia and the locomotor regions. Brain research. 1986; 396:47–63. [PubMed: 2871904]

Garcia-Rill E, Skinner RD, Conrad C, Mosley D, Campbell C. Projections of the mesencephalic locomotor region in the rat. Brain research bulletin. 1986; 17:33–40. [PubMed: 3019486]

Garcia-Rill E, Skinner RD, Miyazato H, Homma Y. Pedunculopontine stimulation induces prolonged activation of pontine reticular neurons. Neuroscience. 2001; 104:455–465. [PubMed: 11377847]

Giber K, Diana MA, Plattner VM, Dugue GP, Bokor H, Rousseau CV, Magloczky Z, Havas L, Hangya B, Wildner H, et al. A subcortical inhibitory signal for behavioral arrest in the thalamus. Nature neuroscience. 2015; 18:562–568. [PubMed: 25706472]

Girard B, Berthoz A. From brainstem to cortex: computational models of saccade generation circuitry. Progress in neurobiology. 2005; 77:215–251. [PubMed: 16343730]

Goldberg JH, Farries MA, Fee MS. Basal ganglia output to the thalamus: still a paradox. Trends Neurosci. 2013; 36:695–705. [PubMed: 24188636]

Grace AA. Dopamine system dysregulation by the ventral subiculum as the common pathophysiological basis for schizophrenia psychosis, psychostimulant abuse, and stress. Neurotoxicity research. 2010; 18:367–376. [PubMed: 20143199]

Grillner S, Hellgren J, Menard A, Saitoh K, Wikstrom MA. Mechanisms for selection of basic motor programs--roles for the striatum and pallidum. Trends in neurosciences. 2005; 28:364–370. [PubMed: 15935487]

Grillner S, Wallen P, Saitoh K, Kozlov A, Robertson B. Neural bases of goal-directed locomotion in vertebrates--an overview. Brain Res Rev. 2008; 57:2–12. [PubMed: 17916382]

Hikosaka O, Nakamura K, Nakahara H. Basal ganglia orient eyes to reward. Journal of neurophysiology. 2006; 95:567–584. [PubMed: 16424448]

Hikosaka O, Takikawa Y, Kawagoe R. Role of the basal ganglia in the control of purposive saccadic eye movements. Physiol Rev. 2000; 80:953–978. [PubMed: 10893428]

Hikosaka O, Wurtz RH. Visual and oculomotor functions of monkey substantia nigra pars reticulata. IV. Relation of substantia nigra to superior colliculus. Journal of neurophysiology. 1983; 49:1285–1301. [PubMed: 6306173]

Kravitz AV, Freeze BS, Parker PR, Kay K, Thwin MT, Deisseroth K, Kreitzer AC. Regulation of parkinsonian motor behaviours by optogenetic control of basal ganglia circuitry. Nature. 2010; 466:622–626. [PubMed: 20613723]

Kreitzer AC, Malenka RC. Striatal plasticity and basal ganglia circuit function. Neuron. 2008; 60:543–554. [PubMed: 19038213]

LeDoux JE. Emotion circuits in the brain. Annu Rev Neurosci. 2000; 23:155–184. [PubMed: 10845062]

Lee AM, Hoy JL, Bonci A, Wilbrecht L, Stryker MP, Niell CM. Identification of a brainstem circuit regulating visual cortical state in parallel with locomotion. Neuron. 2014; 83:455–466. [PubMed: 25033185]

Mamiya K, Bay K, Skinner RD, Garcia-Rill E. Induction of long-lasting depolarization in medioventral medulla neurons by cholinergic input from the pedunculopontine nucleus. Journal of applied physiology. 2005; 99:1127–1137. [PubMed: 15890754]

Martinez-Gonzalez C, Bolam JP, Mena-Segovia J. Topographical organization of the pedunculopontine nucleus. Frontiers in neuroanatomy. 2011; 5:22. [PubMed: 21503154]

Martinez-Gonzalez C, van Andel J, Bolam JP, Mena-Segovia J. Divergent motor projections from the pedunculopontine nucleus are differentially regulated in Parkinsonism. Brain Struct Funct. 2014; 219:1451–1462. [PubMed: 23708060]

Mena-Segovia J, Bolam JP, Magill PJ. Pedunculopontine nucleus and basal ganglia: distant relatives or part of the same family? Trends in neurosciences. 2004; 27:585–588. [PubMed: 15374668]

Mena-Segovia J, Sims HM, Magill PJ, Bolam JP. Cholinergic brainstem neurons modulate cortical gamma activity during slow oscillations. J Physiol. 2008; 586:2947–2960. [PubMed: 18440991]

Mitani A, Ito K, Hallanger AE, Wainer BH, Kataoka K, McCarley RW. Cholinergic projections from the laterodorsal and pedunculopontine tegmental nuclei to the pontine gigantocellular tegmental field in the cat. Brain research. 1988; 451:397–402. [PubMed: 3251602]

Niell CM, Stryker MP. Modulation of visual responses by behavioral state in mouse visual cortex. Neuron. 2010; 65:472–479. [PubMed: 20188652]

Noga BR, Kettler J, Jordan LM. Locomotion produced in mesencephalic cats by injections of putative transmitter substances and antagonists into the medial reticular formation and the pontomedullary locomotor strip. The Journal of neuroscience : the official journal of the Society for Neuroscience. 1988; 8:2074–2086. [PubMed: 2898514]

Norton AB, Jo YS, Clark EW, Taylor CA, Mizumori SJ. Independent neural coding of reward and movement by pedunculopontine tegmental nucleus neurons in freely navigating rats. Eur J Neurosci. 2011; 33:1885–1896. [PubMed: 21395868]

Oldenburg IA, Sabatini BL. Antagonistic but Not Symmetric Regulation of Primary Motor Cortex by Basal Ganglia Direct and Indirect Pathways. Neuron. 2015; 86:1174–1181. [PubMed: 26050037]

Orlovsky GN, Deliagina T, Grillner S. Neuronal Control of Locomotion. From Mollusc to Man. 1999

Perkins E, May PJ, Warren S. Feed-forward and feedback projections of midbrain reticular formation neurons in the cat. Frontiers in neuroanatomy. 2014; 7:55. [PubMed: 24454280]

Redgrave P, Mitchell IJ, Dean P. Descending projections from the superior colliculus in rat: a study using orthograde transport of wheatgerm-agglutinin conjugated horseradish peroxidase. Experimental brain research. 1987; 68:147–167. [PubMed: 2826204]

Ryczko D, Dubuc R. The multifunctional mesencephalic locomotor region. Current pharmaceutical design. 2013; 19:4448–4470. [PubMed: 23360276]

Rye DB, Lee HJ, Saper CB, Wainer BH. Medullary and spinal efferents of the pedunculopontine tegmental nucleus and adjacent mesopontine tegmentum in the rat. The Journal of comparative neurology. 1988; 269:315–341. [PubMed: 2453532]

Saper CB, Swanson LW, Cowan WM. An autoradiographic study of the efferent connections of the lateral hypothalamic area in the rat. The Journal of comparative neurology. 1979; 183:689–706. [PubMed: 105019]

Schiller PH, Stryker M. Single-unit recording and stimulation in superior colliculus of the alert rhesus monkey. Journal of neurophysiology. 1972; 35:915–924. [PubMed: 4631839]

Shang C, Liu Z, Chen Z, Shi Y, Wang Q, Liu S, Li D, Cao P. BRAIN CIRCUITS. A parvalbumin-positive excitatory visual pathway to trigger fear responses in mice. Science. 2015; 348:1472–1477. [PubMed: 26113723]

Sherman D, Fuller PM, Marcus J, Yu J, Zhang P, Chamberlin NL, Saper CB, Lu J. Anatomical Location of the Mesencephalic Locomotor Region and Its Possible Role in Locomotion, Posture, Cataplexy, and Parkinsonism. Frontiers in neurology. 2015; 6:140. [PubMed: 26157418]

Shik ML, Orlovskii GN, Severin FV. Organization of locomotor synergism. Biofizika. 1966a; 11:879–886. [PubMed: 6000596]

Shik ML, Severin FV, Orlovskii GN. Control of walking and running by means of electric stimulation of the midbrain. Biofizika. 1966b; 11:659–666. [PubMed: 6000625]

Sinnamon HM, Ginzburg RN, Kurose GA. Midbrain stimulation in the anesthetized rat: direct locomotor effects and modulation of locomotion produced by hypothalamic stimulation. Neuroscience. 1987; 20:695–707. [PubMed: 3587613]

Skinner RD, Kinjo N, Ishikawa Y, Biedermann JA, Garcia-Rill E. Locomotor projections from the pedunculopontine nucleus to the medioventral medulla. Neuroreport. 1990; 1:207–210. [PubMed: 2129882]

Smetana R, Juvin L, Dubuc R, Alford S. A parallel cholinergic brainstem pathway for enhancing locomotor drive. Nature neuroscience. 2010; 13:731–738. [PubMed: 20473293]

Takakusaki K, Shiroyama T, Yamamoto T, Kitai ST. Cholinergic and noncholinergic tegmental pedunculopontine projection neurons in rats revealed by intracellular labeling. The Journal of comparative neurology. 1996; 371:345–361. [PubMed: 8842892]

Thankachan S, Fuller PM, Lu J. Movement- and behavioral state-dependent activity of pontine reticulospinal neurons. Neuroscience. 2012; 221:125–139. [PubMed: 22796072]

Thompson JA, Felsen G. Activity in mouse pedunculopontine tegmental nucleus reflects action and outcome in a decision-making task. Journal of neurophysiology. 2013; 110:2817–2829. [PubMed: 24089397]

Van Dort CJ, Zachs DP, Kenny JD, Zheng S, Goldblum RR, Gelwan NA, Ramos DM, Nolan MA, Wang K, Weng FJ, et al. Optogenetic activation of cholinergic neurons in the PPT or LDT induces REM sleep. Proceedings of the National Academy of Sciences of the United States of America. 2015; 112:584–589. [PubMed: 25548191]

Wall NR, De La Parra M, Callaway EM, Kreitzer AC. Differential innervation of direct- and indirect-pathway striatal projection neurons. Neuron. 2013; 79:347–360. [PubMed: 23810541]

Whelan PJ. Control of locomotion in the decerebrate cat. Progress in neurobiology. 1996; 49:481–515. [PubMed: 8895997]

Zhao S, Ting JT, Atallah HE, Qiu L, Tan J, Gloss B, Augustine GJ, Deisseroth K, Luo M, Graybiel AM, et al. Cell type-specific channelrhodopsin-2 transgenic mice for optogenetic dissection of neural circuitry function. Nature methods. 2011; 8:745–752. [PubMed: 21985008]

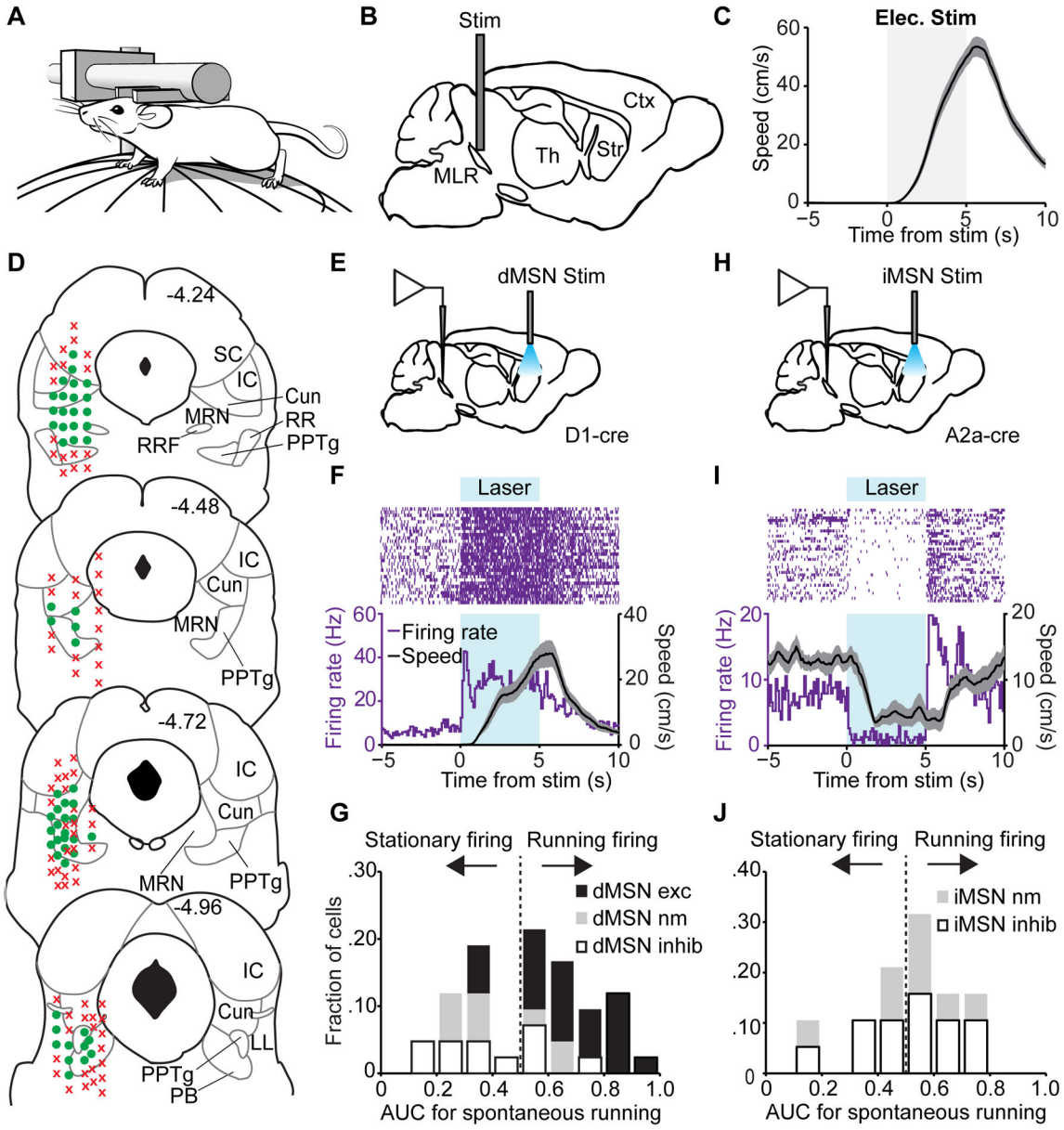

Figure 1. Mapping and bidirectional BG regulation of the MLR

(A) Illustration of head-fixed trackball setup. **(B)** Schematic of stimulation within the MLR. **(C)** Population time course for mouse speed aligned to 20 Hz electrical stimulation (n = 7 mice). **(D)** MLR mapping using electrical stimulation. Green circles represent electrode placement at which stimulation elicited locomotion (> 5 cm/s) with short latency (< 2 s), red X's represent electrode placement where no running was observed. SC, superior colliculus; IC, inferior colliculus; Cun, cuneiform nucleus; RRF, retrorubral field; MRN, mesencephalic reticular nucleus; RR, retrorubral nucleus; PPTg, pedunculopontine tegmentum; LL, lateral lemniscus; PB, parabrachial nucleus (n = 13 mice). **(E)** Schematic for stimulation of striatal dMSNs while recording activity in the MLR. **(F)** Example neuron excited during dMSN stimulation. Top, rasters of individual trials; bottom, peri-event time

histogram (PSTH) of firing rate (purple line) and mouse speed (black line) aligned to onset of stimulation. **(G)** Histogram of AUCs for speed vs firing rate during a spontaneous locomotor session after dMSN stimulation. Black bars, neurons excited by dMSN stimulation ("dMSN exc"); gray bars, neurons unmodulated by dMSN stimulation ("dMSN nm"); open bars, neurons inhibited by dMSN stimulation ("dMSN inhib"), (n = 42 neurons from 4 mice). **(H)** Schematic for stimulation of striatal iMSNs while recording activity in the MLR. **(I)** Example neuron inhibited during iMSN stimulation as in (F). **(J)** Histogram of AUCs for speed vs firing rate during a spontaneous locomotor session after iMSN stimulation. Gray bars, neurons unmodulated by iMSN stimulation ("iMSN nm"); open bars, neurons inhibited by iMSN stimulation ("iMSN inhib"), (n = 26 neurons from 4 mice). All shaded regions, s.e.m.

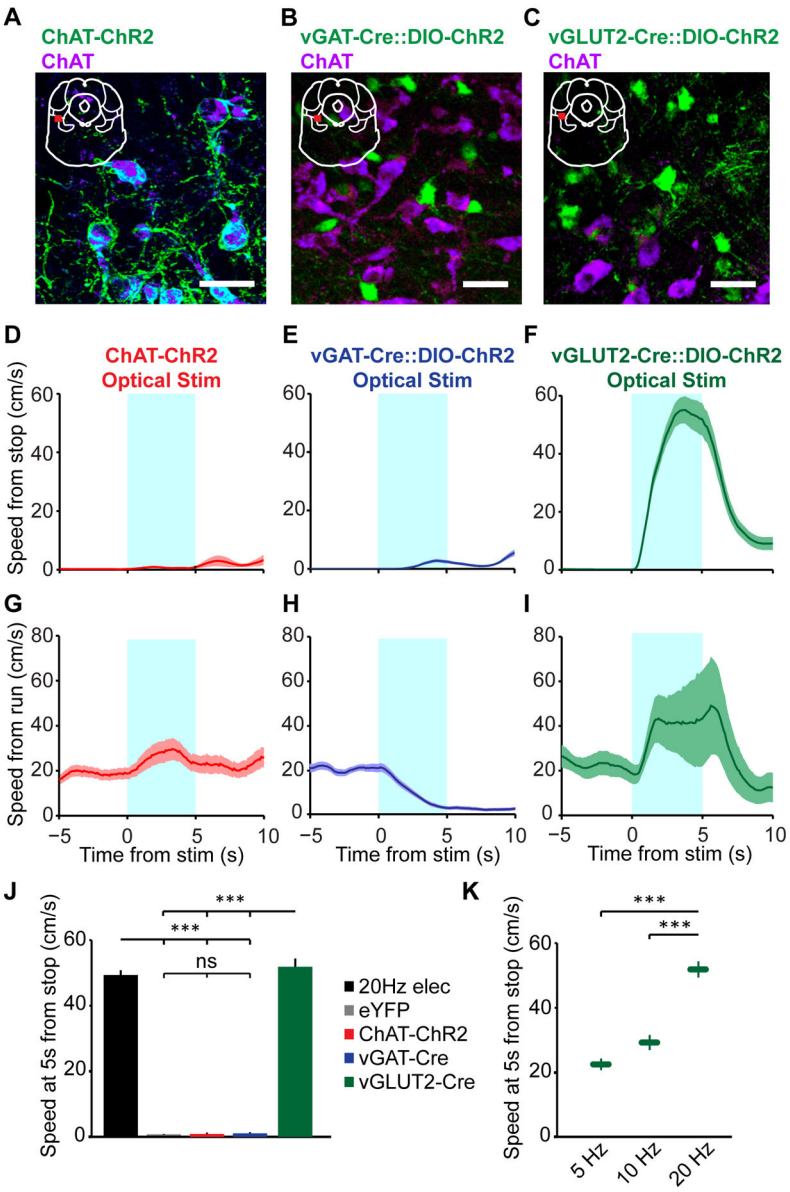

Figure 2. Distinct functions of MLR cell types

(A–C) Confocal images of coronal sections through the MLR of ChAT-ChR2 (A), vGAT-Cre::DIO-ChR2 (B) and vGLUT2-Cre::DIO-ChR2 (C) counter stained for ChAT, which demarcates the boundaries of the PPTg. Insets show location of image. (scale bar 25 μm) **(D–I)** Population time course for mouse speed aligned to 20 Hz optical stimulation from stationary (D–F) and running (G–I) states, in ChAT-ChR2 mice (D, G; n = 5 mice, 7 hemispheres), vGAT-Cre::DIO-ChR2 mice (E, H; n = 4 mice, 6 hemispheres) and vGLUT2-Cre::DIO-ChR2 mice (F, I; n = 6 mice, 7 hemispheres). Shaded regions, s.e.m. **(J)** Summary of population speed at 5 s after stimulation onset (*** $p < 10^{-4}$, Kruskal-Wallis one-way ANOVA, $\chi^2_{3,243} = 175.52$, $p < 10^{-10}$, with Dunn-Sidak post test). **(K)** Summary of speed at 5 s during graded stimulation of glutamatergic neurons (*** $p < 10^{-4}$, Kruskal-Wallis one-

way ANOVA, $\chi^2_{2,167} = 175.52$, $p < 10^{-5}$, with Dunn-Sidak post test). All shaded regions, s.e.m. See also Figures S1 and S2.

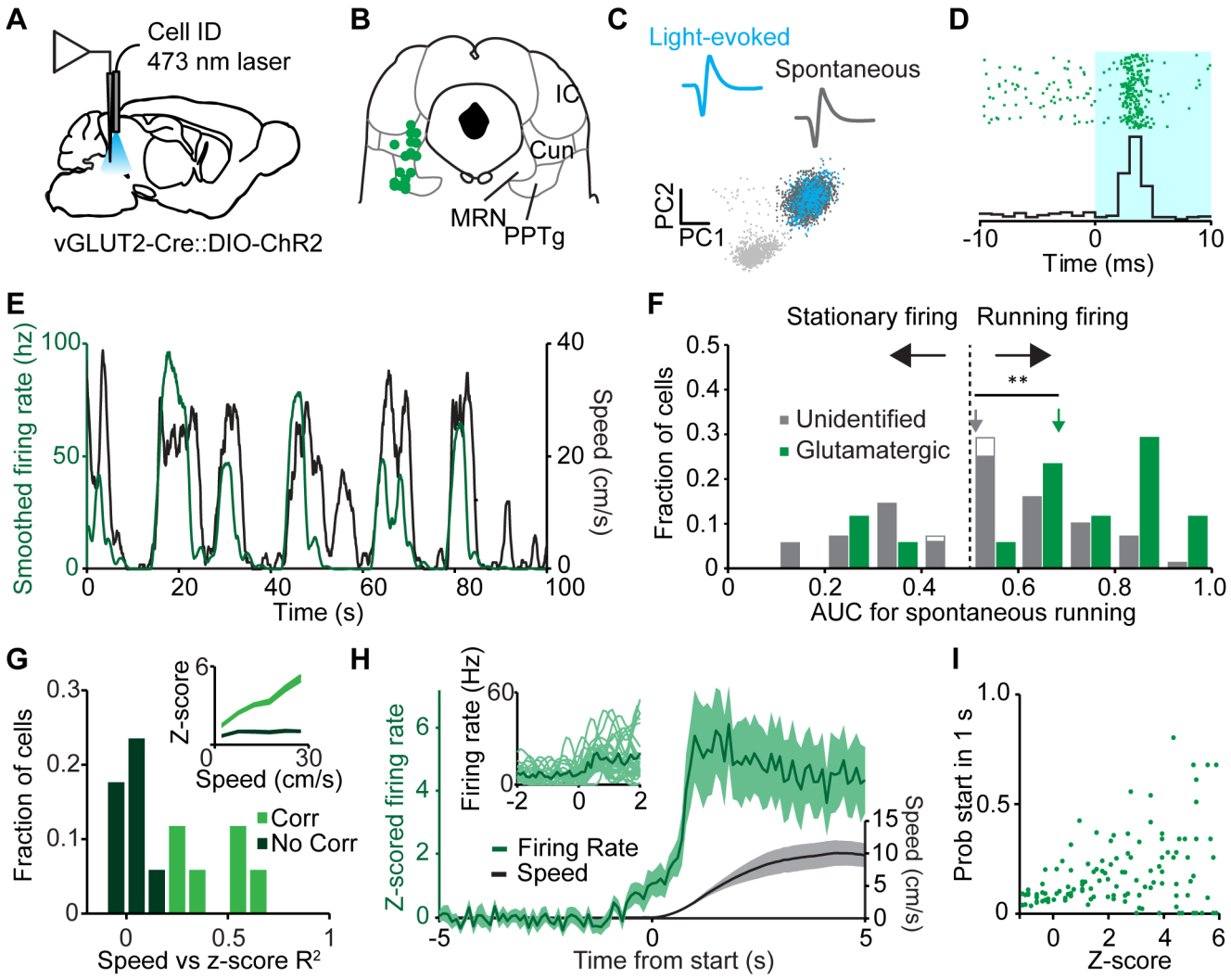

Figure 3. Characterization of MLR glutamatergic neurons

(A) Schematic of optical tagging and recording setup in vGLUT2-Cre::DIO-ChR2 mice. **(B)** Recording sites for ChR2-positive (glutamatergic) neurons. **(C)** Top, light-evoked and spontaneous waveforms of an identified neuron. Bottom, PC1 vs PC2 for the neuron. Light gray dots, noise; dark gray dots, spontaneous spikes; blue dots, light-evoked spikes. **(D)** Raster (top) and PSTH (bottom) for a light-reactive neuron showing 3 ms latency aligned to laser onset. **(E)** Smoothed firing rate of the neuron identified in (C) and (D) (green line, left axis) plotted with the speed of the mouse (black line, right axis). **(F)** Histogram of AUC's for all recorded neurons during spontaneous locomotion. Green bars, identified glutamatergic neurons (all significantly encoded the stationary or locomotor state); filled grey bars, unidentified neurons recorded in the MLR from a separate cohort that significantly encoded the stationary or running state; open grey bars represent neurons which did not significantly encode either state. Arrows, means; ** $p < 0.001$, Wilcoxon rank sum. **(G)** Histogram of R^2 values for the glutamatergic neurons that predicted locomotion in (F) (n = 14). Light green bars, speed correlated neurons; dark green bars, neurons not correlated with speed. **(H)** Population z-scored firing rate of identified glutamatergic

neurons (green trace) aligned to onset of locomotion. Black trace, speed. Inset, individual example firing rate traces (light green) and average (dark green) aligned to starts. **(I)** Probability of a start within one second given z-scored firing rate. Each point represents one binned data point (0.1 sd bins) from one neuron. All shaded regions, s.e.m. See also Figure S3.

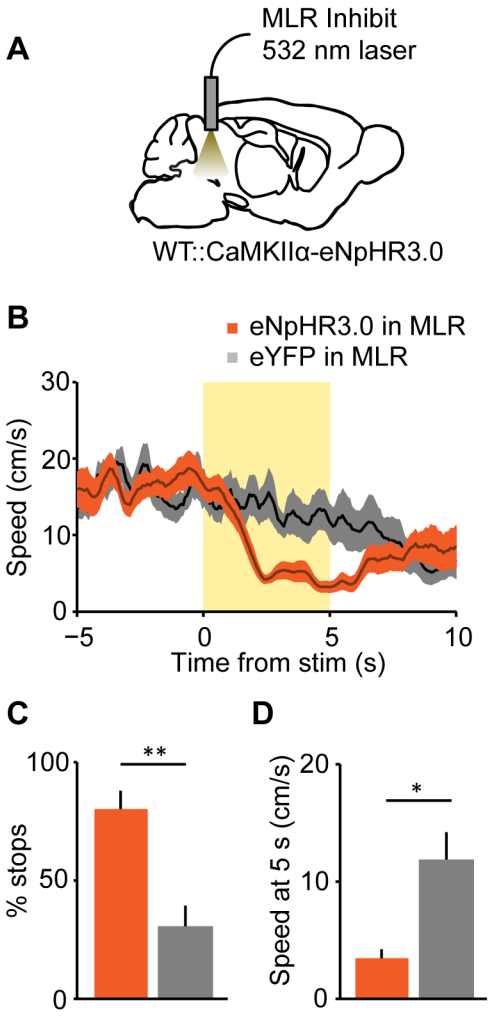

Figure 4. Inhibition of MLR glutamatergic neurons impedes running

(A) Experimental schematic for inhibiting glutamatergic neurons in the MLR. **(B)** Speed aligned to laser onset, or with no stimulation (eNpHR3.0 in MLR, orange line, n = 4 mice; eYFP in MLR, black line, n = 6 mice). **(C)** Number of stops during laser inhibition for each group. **(D)** Speed summary data at 5 seconds after onset of laser inhibition. * $p < 0.05$, ** $p < 0.01$, Wilcoxon rank sum. Shaded regions, s.e.m.

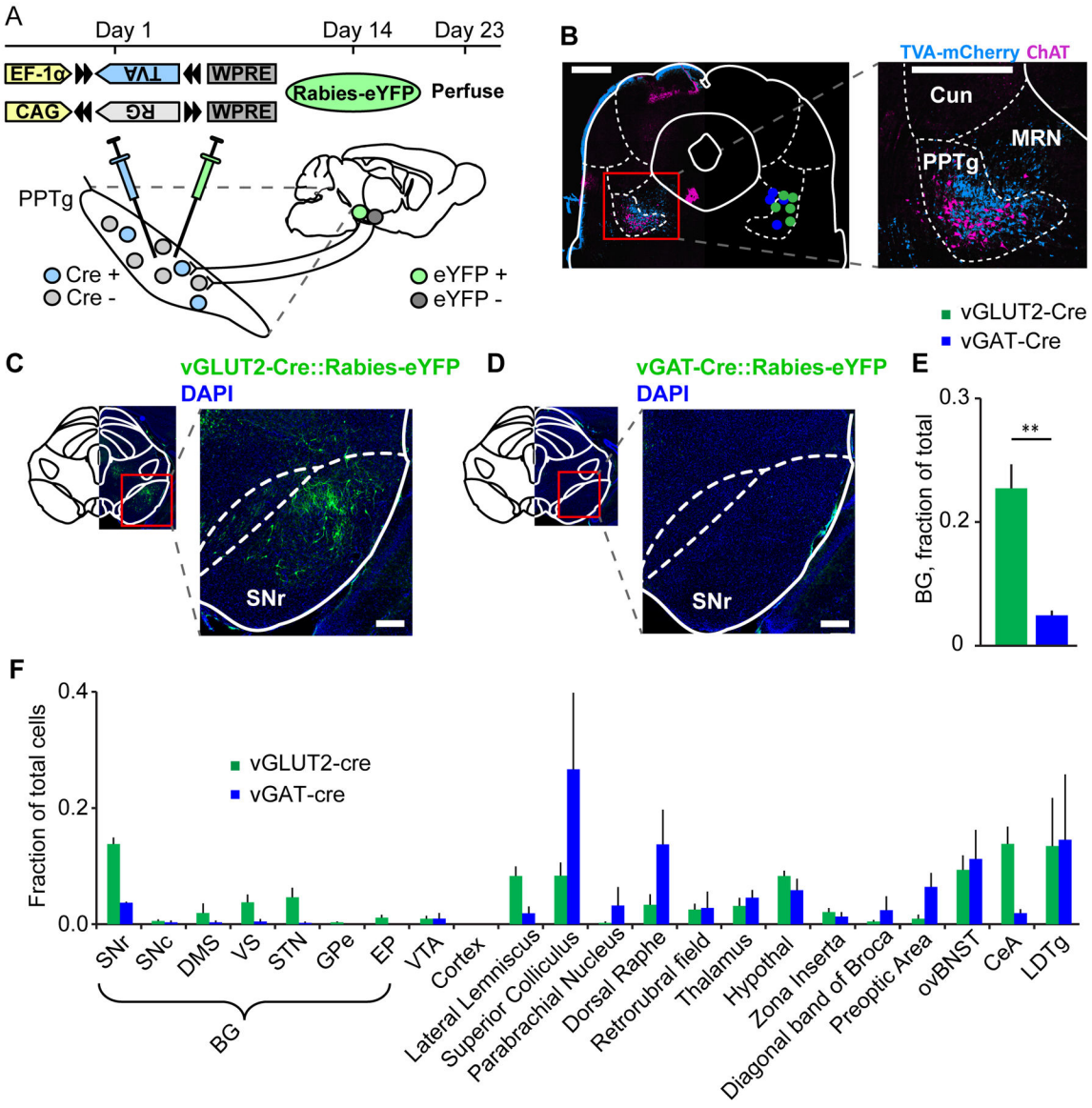

Figure 5. Brain-wide mapping of inputs to MLR glutamatergic and GABAergic neurons

(A) Schematic and time course of experiment. **(B)** Left, coronal section through the MLR showing TVA-mCherry labeling (blue) around the PPTg (labelled with ChAT staining, pink) and center-of-mass of TVA and RG injection sites. (red dots, vGAT-Cre::TVA+RG; green X's, vGLUT2-Cre::TVA+RG). Right, close-up of infected cells. Scale bars, 500 μm. **(C–D)** Examples of eYFP expression in the SNr in a vGLUT2-Cre::Rabies-eYFP (C) and vGAT-Cre::Rabies-eYFP (D). Scale bars, 200 μm. **(E)** Quantification of labelled cell counts from all BG nuclei in vGLUT2-Cre::Rabies-eYFP (green bars) and vGAT-Cre::Rabies-eYFP mice (blue bars). ** $p < 0.01$, Wilcoxon rank sum. **(F)** Quantification of ipsilateral inputs to MLR glutamatergic (green) and GABAergic (blue) neurons. SNr, substantia nigra pars reticulate; SNc, substantia nigra pars compacta; DMS, dorsomedial striatum; VS, ventral striatum; STN, subthalamic nucleus; GPe, external globus pallidus; EP,

entopeduncular nucleus; VTA, ventral tegmental area; CeA, central amygdalar nucleus; LDTg, laterodorsal tegmental nucleus. Error bars, s.e.m.

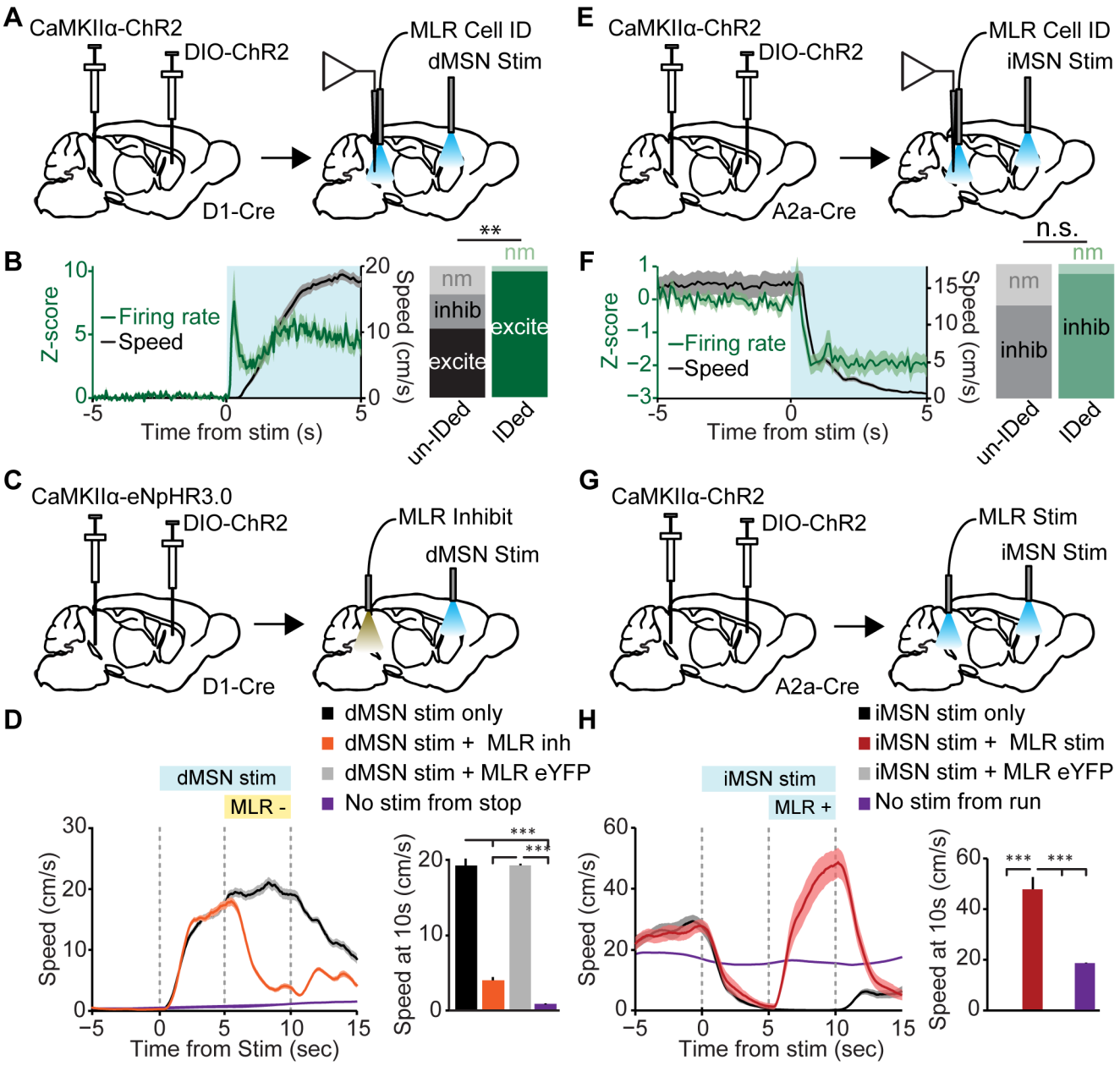

Figure 6. MLR glutamatergic neurons are necessary and sufficient to reverse the effects of BG stimulation

(A) Schematic for recording MLR glutamatergic neurons, while activating dMSNs in striatum. **(B)** Left, Z-scored firing rate of identified glutamatergic neurons (green line, left axis) and speed (black line, right axis) aligned to onset of 5 second unilateral dMSN stimulation from stop. Right, fractions of excited (excite), inhibited (inhib), or non-modulated (nm) units in unidentified recordings (un-IDed, left) and in identified glutamatergic cells (IDed, right). (identified: 25 excited, 0 inhibited, 1 non-modulated from 4 mice; unidentified: 22 excited, 11 inhibited, 9 non-modulated from 4 mice; ** $p < 0.001$, χ^2 test). **(C)** Schematic for stimulating dMSNs in striatum, while inhibiting MLR

glutamatergic neurons. **(D)** Left, Speed aligned to unilateral dMSN stimulation. Orange line, trials in which green light was turned on in the MLR 5 seconds after dMSN stimulation; black line, interleaved trials in which green light was omitted; purple line, no stimulation trials when mouse is stopped. Right, Speed 10 seconds after onset of dMSN stimulation (*** $p < 10^{-4}$, Kruskal-Wallis one-way ANOVA, $\chi^2_{3,136} = 92.35$, $p < 10^{-10}$, with Dunn-Sidak post test). **(E)** Schematic for recording identified MLR glutamatergic neurons, while activating iMSNs in striatum. **(F)** Left, Z-scored firing rate of glutamatergic neurons (green line, left axis) and speed (black line, right axis) aligned to onset of 5 second bilateral iMSN stimulation from running. Right, summaries for the number of inhibited (inhib) or non-modulated (nm) units in unidentified (unIDed, left) recordings and identified (IDed, right) glutamatergic neurons (identified: 25 inhibited, 2 unmodulated from 4 mice; unidentified: 18 inhibited, 8 unmodulated from 3 mice; $p = 0.09$, χ^2 test). **(G)** Schematic for stimulating iMSNs in striatum while stimulating glutamatergic cells in the MLR. **(H)** Left, time course of mouse speed aligned to bilateral iMSN stimulation. Red line, trials in which blue light was turned on in the MLR at 20 Hz 5 seconds after iMSN stimulation; black line, interleaved trials in which green light was omitted; purple line, no stimulation trials when mouse is running. Right, summary of mouse speed 10 seconds after onset of iMSN stimulation (*** $p < 10^{-4}$, Kruskal-Wallis one-way ANOVA, $\chi^2_{3,105} = 75.06$, $p < 10^{-10}$, with Dunn-Sidak post test). Shaded regions, s.e.m. See also Figures S5 and S6.